JOURNAL OF PROPULSION AND POWER
Vol. 18, No. 4, July–August 2002

Development and Flight Qualification of a 26-Kilowatt Arcjet Propulsion Subsystem

R. J. Cassady,* W. A. Hoskins,† and C. E. Vaughan‡
General Dynamics Corporation, Redmond, Washington 98073

The Electric Propulsion Space Experiment (ESEX) flew in 1999 on the Air Force Space Test Program Advanced Research and Global Observation Satellite. ESEX was initiated to address potential in-space operational issues associated with the use of high-power electric propulsion. Potential issues included plume deposition, electromagnetic interference, and thermal radiation. Because of physical constraints of even the largest test facilities, that is, vacuum chamber size, these phenomena are best measured in space. The propulsion component for the ESEX demonstration, a 26-kW ammonia arcjet propulsion subsystem, including thruster, power processing, and propellant feed, was developed and flight qualified on the Air Force Research Laboratory Arcjet Advanced Technology Transition Demonstration program. Each of the propulsion system elements, the principal design challenges, and the program of risk reduction and qualification testing that provided preflight verification of the arcjet propulsion subsystem are described.

Introduction

THE Electric Propulsion Space Experiment (ESEX)[1] was conceived to be a demonstration of a complete high-power, electric propulsion system in the space environment, with associated diagnostics to record the key operating parameters and to perform in-situ measurements. ESEX was configured to fly as part of the Space Test Program's P91-1 Advanced Research and Global Observation Satellite (ARGOS). ESEX depended on ARGOS for attitude control, battery recharge, housekeeping power, telemetry, and commands. Beyond this host vehicle support, ESEX was designed to perform arcjet firings independently and to collect an array of data designed to characterize the interaction of the high-power arcjet system with the spacecraft. The goal of the mission was to perform 10 arcjet firings of approximately 15 min duration. To perform such high-power steady state firings with the limited electrical power available from ARGOS, the ESEX system included a silver–zinc battery pack capable of providing 6780 W · h/15-min arcjet firing. For each arcjet firing, 100 h were allocated. The batteries were charged over a 60–70 h period before the arcjet firing. Just after the completion of the firing, the battery pack entered a cool-down mode for approximately 20–30 h. The battery pack was then recharged and the cycle repeated. The actual timing of the firings was coordinated to allow for observation from and communication with various Air Force ground stations. The entire ESEX payload is described in more detail in Ref. 2.

Within ESEX, power to the various subsystems was distributed and controlled by the power integration unit (PIU). Command and data handling were provided by the command/control unit. Diagnostic equipment included a camera, solar cell samples, thermal quartz crystal microbalances, a radiometer, and an electromagnetic interference (EMI) antenna boom. The arcjet propulsion subsystem, described herein, consisted of the arcjet thruster and cable, a 30-kW class power conditioning unit (PCU) to condition battery output into the power required by the arcjet, and a propellant feed subsystem (PFS) to provide ammonia to the arcjet at a controlled flow rate.

Received 15 June 2001; revision received 24 December 2001; accepted for publication 27 January 2002.

*Senior Manager, Business Development Space Propulsion Systems. Member AIAA.
†Project Engineer, Space Propulsion Systems. Member AIAA.
‡Director, Space Systems Engineering, Space Propulsion Systems.

Arcjet Propulsion Subsystem Design

Development of the 26-Kilowatt Ammonia Arcjet Thruster

Before the ESEX development under the Arcjet Advanced Technology Transition Demonstration (Arcjet ATTD) Program, several arcjet development activities had been conducted at the 10–30 kW power level.[3,4] The common element of all of these efforts was the focus on performance and lifetime of the arcjet. The development arcjets were laboratory models utilizing bolt-together assemblies that allowed for disassembly and replacement of internal parts. Therefore, they were unsuitable for flight application. The challenge to transition the successful laboratory thruster designs to a flight design revolved principally around issues such as thermal rejection of waste heat, structural integrity under launch loads, and sealing and materials joining techniques.

Analysis of the arcjet showed that, although the overall efficiency was only 30%, the thermal efficiency (thermal energy delivered to the effluent divided by input power) was much closer to 90% of the power delivered to the arcjet. However, this still meant that approximately 3000 W had to be dissipated. The design goal was to minimize the conducted heat back into the spacecraft, and so a long thermal barrier tube was employed. To maximize the amount of heat radiated from the arcjet, a high-emissivity coating was applied to the anode. A special thermal shield was designed to shadow the components on the ESEX deck from the directly radiated energy. The lengthened design of the arcjet (more than twice as long as the laboratory models), combined with the heavy tungsten anode at the end of the barrier tube, drove the structural and mounting design to a larger diameter cylindrical structural cage. The resultant design of the 26-kW arcjet was similar to, but much larger than, the 2-kW class arcjets now routinely flown on commercial communications satellite.

Sealing and joining the various elements of the arcjet presented its own set of problems. Combining the requirements to conduct currents of up to 250 A, to withstand at least a 6000-V start pulse, to join structurally ceramics to metals, and to maintain permanent hermetic seals comprised a very difficult engineering problem. A critical component of every flight arcjet is the hermetically sealed power connector on the upstream side of the arcjet. In addition, a cable had to couple the 30 kW of electrical energy from the PCU into the arcjet. Ultimately, a custom power connector and cable was developed because nothing was commercially available that satisfied the requirements. The cable assembly used a triaxial copper bus

bar with spiral machined slots for strain relief, which also served to minimize radiated electromagnetic emissions. The inner conductor carried the high-voltage cathode current, the inner shield provided anode return, and the outer shield constituted an EMI barrier, grounded both at the PCU chassis and the arcjet body mount. The fully integrated arcjet with cable is shown in Fig. 1.

The thruster design had to withstand internal temperatures in excess of 1100°C at one end of the propellant manifold, while maintaining a temperature near 100°C at the spacecraft interface. Inside the arcjet, the electrodes were electrically isolated using ceramic insulators that were restrained to protect them during launch vibrations, while allowing them to accommodate thermal expansions through a complex series of high-temperature loading elements. For the anode and thruster body, a joining system was devised that involved a leak tight press-fit of the tungsten anode into a molybdenum rhenium alloy sleeve that could be welded to the molybdenum rhenium alloy transition tube, which was in turn brazed to the Inconel main structure. The design solution to these requirements has been described in detail in earlier papers[5] and is shown in Fig. 1.

Development of the 30-Kilowatt Class PCU

The Arcjet ATTD Program required the design, fabrication, test, and operation of a 30-kW class PCU to condition the battery power to the startup, rampup, and steady-state voltages and currents required by the arcjet. To maximize reliability and efficiency, which in turn limited the thermal load into the ESEX payload, the PCU used a buck regulator topology of three switching phases offset by 120 deg to minimize current ripple. As with the arcjet, work had been done under previous contracts to develop the basic concept of the 30-kW class PCU. Earlier work pioneered the concept of using a three-phase buck regulator approach.[6]

The major challenges to obtain a flight design were to package the three buck regulator phases into an integrated design with good thermal pathways to dissipate heat, controlling EMI/electromagnetic compatibility (EMC), adding logic, telemetry, and control circuits and minimizing size and mass. Operationally, the PCU received power from the ESEX batteries. The PCU received command inputs from, provided PCU status to, and conditioned transducer signals (pressure, temperature, voltage, and current) to the ESEX CCU. The PCU also controlled the operation of the arcjet inlet valve to provide propellant to the arcjet thruster during firing periods.

To initiate the thruster arc, the PCU produced a 1.5-μs, 6000-V (or greater) pulse. After arc initiation, the PCU maintained a constant thruster warmup current of about 85 A (a power of about 10 kW) for approximately 10 s. To minimize temperature gradients in the arcjet, the PCU then ramped up the output current at a nominal 10-kW/min rate to a 26-kW output power level that was maintained for the remainder of the 15-min firing.

The principal performance characteristics of the PCU are summarized in Table 1, and the PCU is shown in Fig. 2 (Ref. 5). Important features of the design implementation included the use of low-mass, high-efficiency hybrid field-effect transistor (FET) switches in the converter and bonding of those switches directly to the baseplate for optimum thermal dissipation. The use of parallel plane bus bars minimized EMI effects within the enclosure, whereas the command and control card cages were isolated from radiated EMI from the power converter by internal bulkheads.

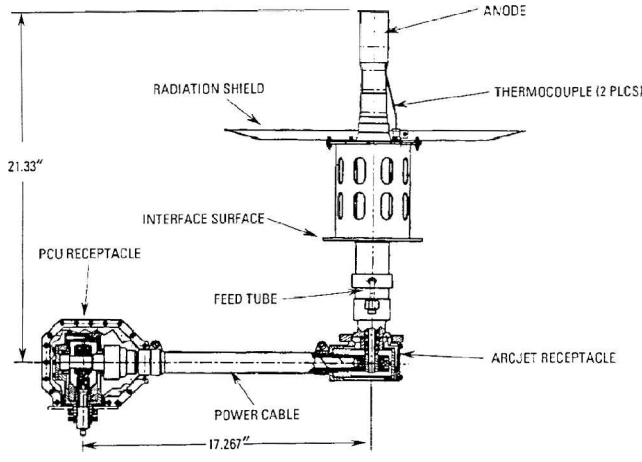

Fig. 1 Arcjet and power cable in integrated configuration.

Table 1 PCU requirements summary

Parameter	Value
Input power	160 – 240 Vdc (main power) +28 Vdc (auxiliary power)
Output to arcjet thruster	90 – 130 Vdc 26,000 ± 370 W steady state
Output ripple current	15% peak–peak
Arcjet thruster start voltage	5000 ± 1000 Vdc (1.5 μs duration)
Efficiency	95%
Dynamic regulation	10-A output current change for step load change of 0.05 Ω
Envelope	46.74 cm × 60.96 cm × 15.24 cm (18.4 in. × 24.0 in. × 6.0 in.)
Mass	48.4 kg (107 lbm)
Reliability	15,000 h mean time between failures (per MIL-HDBK-217E)
Mounting surface temperature	−29 to +55°C (on-orbit)
Pressure	1.3×10^{-4} Pa (10^{-6} torr) orbit ⟨0.13 Pa or⟩ 5.3 kPa (⟨10^{-3} torr or⟩ 40 torr) test
Acceleration	10 g (X, Y, Z axes)
Vibration	9.3 g rms (X, Y, Z axes)
Launch shock	1500 g
Radiation	10 rad (200 n mile orbit altitude)
EMI	MIL-STD-461C. Category A2a (tailored)

At a 30-kW power level, the thermal design challenge was significant because ARGOS was only capable of accepting a few hundred watts for a short period of time. However, when the efficiency was maintained at over 96%, the dissipated power was limited to a total of 1024 W. This allowed the use of a passive aluminum heat sink to maintain the baseplate temperature at less than 55°C following a 15-min firing. Because of the silver–zinc battery power source, the design had to work with an input voltage variation from 240 down to 160 V dc, while providing a constant power output to the thruster. With an overall mass of approximately 48.5 kg, the power density was 1.62 kg/kW at the full rated power of 30 kW, compared with 3.64 kg/kW for the arcjet PCU flown on commercial A2100™ satellites.[7] Power densities for other electric propulsion systems include the RHETT Hall thruster power processing unit (PPU) at 10 kg/kW (Ref. 8) and the NASA Solar Electric Propulsion Technology Application Readiness ion engine PPU at 5.27 kg/kW (Ref. 9).

At the outset, the Arcjet ATTD Program did not include the development of a new start circuit. The original intent was to adapt an existing circuit concept into a flight design. However, early in the program, concerns were raised about the adequacy of the 2500-V start circuit from early PCU efforts.[10] The arc breakdown phenomenon for 30-kW class ammonia arcjets had been poorly characterized, and as more data were produced, it was clear that a departure from the baseline start circuit was required to ignite to the arcjet reliably.

To overcome the deficiencies of the baseline start-circuit design a pulser-circuit approach was employed that contained a flyback inductor connected in parallel with the output of the converters. Figure 3 is a simplified schematic of the flight circuit.[11] When the 500-V switch on the primary of the flyback is opened after charging the circuit, the output flies back at a 12:1 ratio. The 500 V Zener diode in parallel with the switch limits the output nominally to at least 6,000 V, although parasitic inductance actually allowed somewhat higher voltages (6,000–10,000 V).

A key to the implementation of the circuit was the addition of 9-mH blocking inductors on the output of the converters. These inductors act as a magnetic switch, appearing as an open circuit during the fast rising start pulse. Without this open switch, the pulse energy would merely dissipate back through the converters instead of being applied to the arcjet electrodes. Large output diodes could have

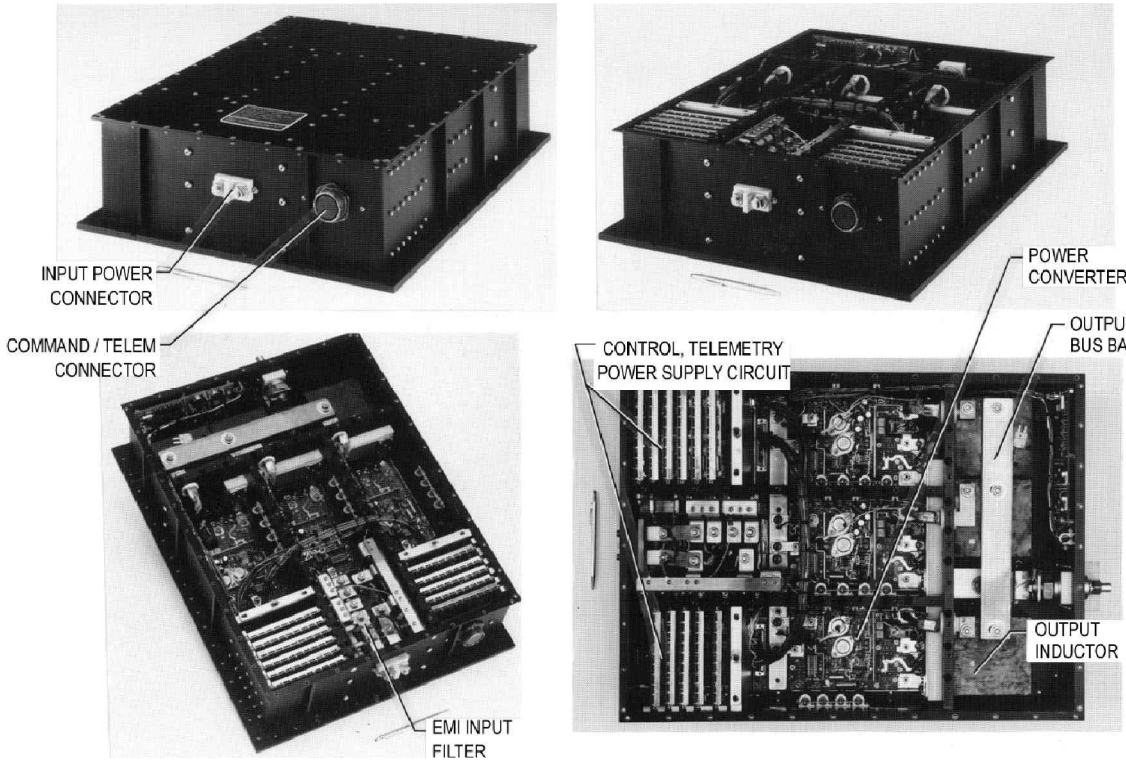

Fig. 2 PCU of 30 kW.

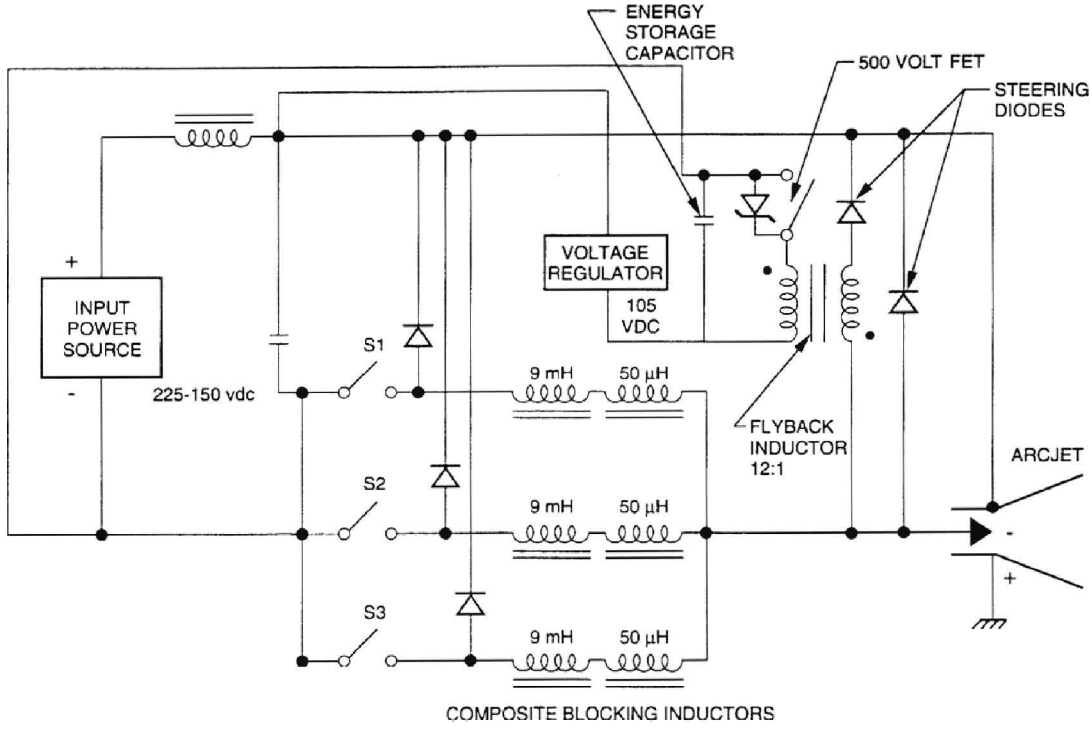

Fig. 3 Start-circuit schematic.

accomplished the same function, but the energy loss for the output current at 26 kW would have been unacceptable. When the arcjet breaks down, current from the start circuit sustains the incipient arc for on the order of 100 μs. After this time, which is a function of the integral of voltage and time, the blocking inductor reaches a designed saturation limit and closes as a switch, allowing forward conduction of the primary current from the power converters.

Development of the Ammonia PFS

The original project plan was to duplicate the ammonia feed system that had flown on the Lincoln Laboratories experimental satellite (LES) 8/9 spacecraft. The use of this system was precluded by lack of availability of components, lack of manufacturing instructions, and the extremely precise flow tolerances required for arcjet operation. Consequently, the system requirements were reevaluated to identify an alternate solution.[12]

The arcjet ATTD mission required a total of 10, 15-min ammonia outflows at 240 ± 5 mg/s. In addition, the PFS had to be low cost, and so new component development was very limited. An immediate issue was to provide an ammonia vaporization system that would allow precision flow control of $\pm 2\%$, would accept any phase of tank outflow ranging from saturated liquid to saturated vapor, and,

finally, would function in any orientation in 1-*g* test, as well as 0-*g* orbital environments. Because a propellant management device was not used, a packed bed vaporizer was developed to guarantee that only gas-phase propellant would reach the arcjet. Experimental work confirmed that a packed bed vaporizer with a power input of about 500 W would meet these requirements. Experimental work also revealed that the zone of vaporization oscillated through the entire 150 cm length of the packed bed. This phenomenon had the potential to wash out the vaporizer, thereby introducing liquid ammonia into the arcjet. To eliminate this possibility, a control algorithm for the two segments of the vaporizer heater and the control valve was developed. The resulting bang–bang system controlled flow rate by varying the open time for a 2-Hz-cycle valve pulsing frequency at the outlet of the vaporizer. The outflow of the vaporizer pressurized a plenum tank upstream of a sonic venturi orifice; the plenum volume provided a capacitance to reduce cyclic variation in the flow. Flow rate was measured by temperature and pressure just upstream of the orifice and provided feedback to the control algorithm.

Heaters on the propellant tank were located and operated to maintain the outlet pole of the tank above the boiling point of ammonia. The intent was to thermally pump liquid ammonia away from the outlet so that a higher power vaporizer would not be required. Because ammonia has a meniscus contact angle of essentially 0 deg, a thin film of ammonia was expected to wet the tank surface by capillary forces. The tank outlet was also oriented so that the acceleration generated during arcjet thrusting would move liquid away from the outlet. Marangoni flow (see Ref. 13) and the use of the dynamic Bond number (see Ref. 14) improved the performance further by allowing continuous gas outflow without demanding the 500 W needed to power the vaporizer. Ground testing in 1 *g* could not validate the performance of this thermocapillary behavior. The inability to perform a preflight validation was the principal reason to include a vaporizer in the PFS.

The system is shown schematically in Fig. 4, and a diagram of the physical layout is shown in Fig. 5. The use of qualified existing components for tanks, pressure transducers, valves, and immersion

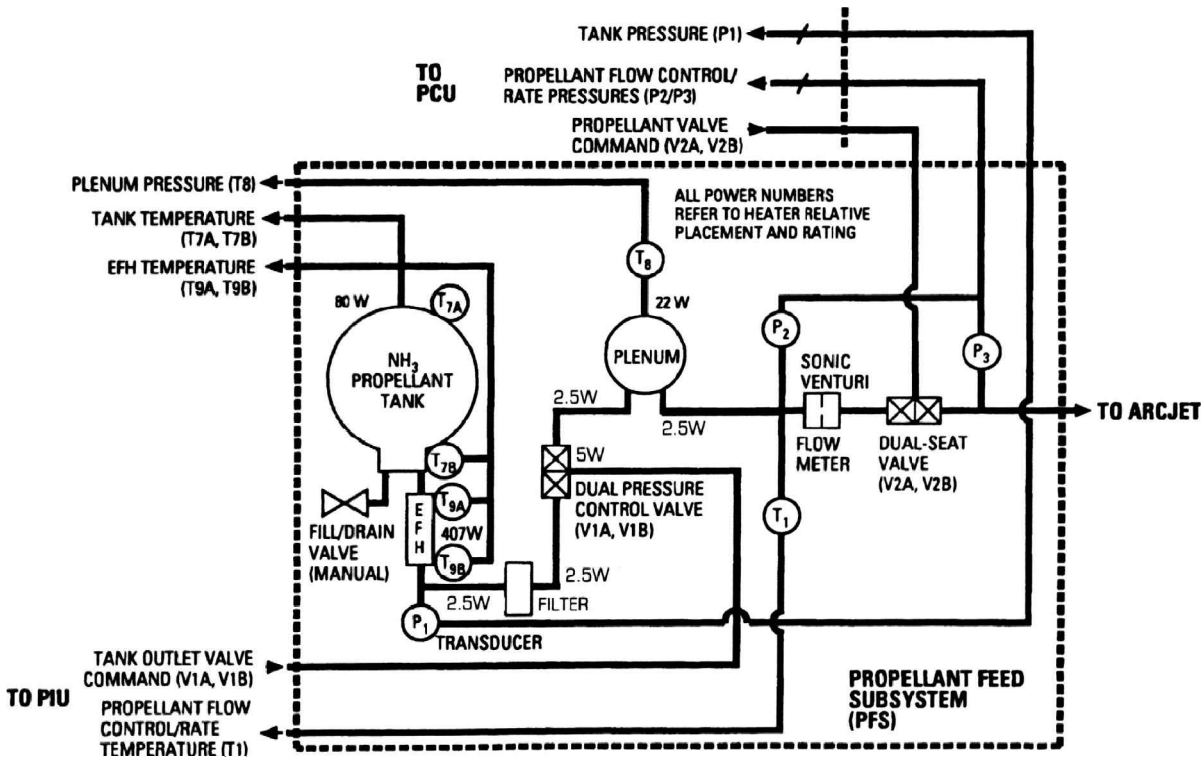

Fig. 4 PFS schematic.

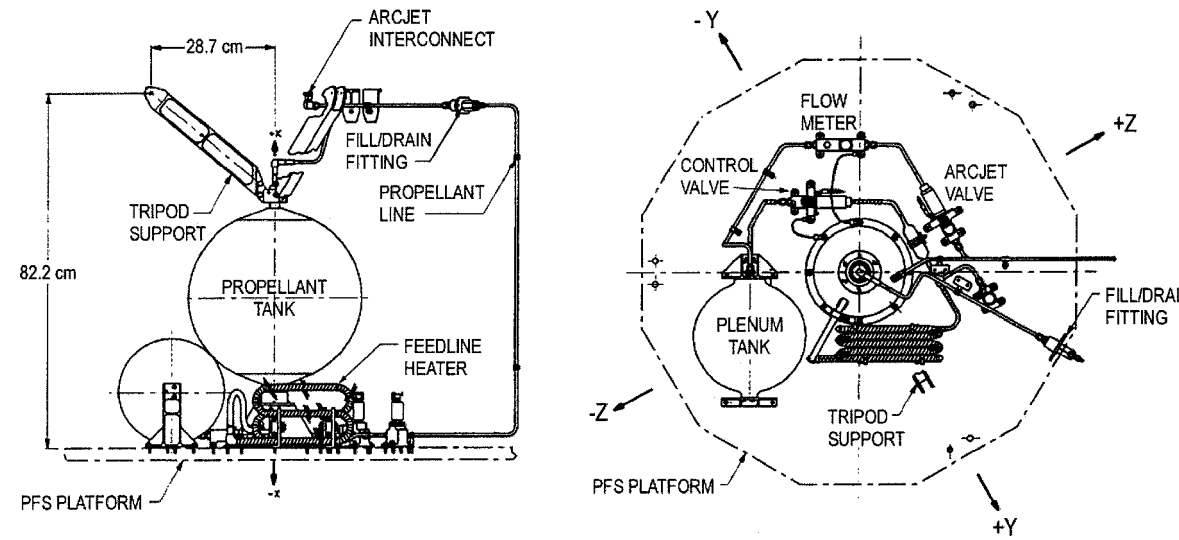

Fig. 5 PFS design details.

thermocouples helped maintain an overall low cost for the subsystem. The ground and flight testing demonstrated that the vaporizer delivered continuous, high-quality (superheated) vapor to the thruster at a high overall efficiency. The digital control system demonstrated precise mass flow control with better than ±1.5% flow variation. The system was capable of continuous gas-phase outflows regardless of orientation in 1 *g* or 0 *g* or of inlet propellant phase. The in-flight power profile of the vaporizer proved that no liquid was exiting the tank outlet, thereby confirming that thermocapillary forces can be used to supply single-phase flow from a propellant tank without a propellant management device. Features of this subsystem could be incorporated into other propellant feed systems for electric or low-thrust chemical propulsion missions including systems using thrusters other than arcjets or propellants other than ammonia.

Testing Program

The ATTD testing program was planned to reduce risk early, to verify the stable, integrated operation of all of the major propulsion subsystem components, and to speed the development cycle by eliminating a separate qualification phase.[15,16] Whereas the arcjet thruster electrode configuration had been defined and the performance demonstrated before the ATTD program,[3] major features, such as the PCU start circuit and the entire PFS concept were undemonstrated at the start of the program. In addition, although 30-kW class arcjets had been tested for three decades before this time, this testing had been performed with laboratory power supplies, and simple, gas bottle propellant feed systems. Never before had controlled ammonia feed system or a flight configuration PCU been connected to a 30-kW arcjet with a battery power source. To allow elimination of a qualification phase with separate qualification hardware, the engineering model (EM) hardware was very flight-like, the key integrated tests were conducted during the EM phase, and the combination of EM and flight unit testing comprised the full flight qualification of the unit. In summary, this test program was the first example of an end-to-end ground verification of a major electric propulsion system with flight design propellant subsystem components to validate their selection.

Development Testing

The arcjet thruster performance had been tested extensively under such programs as the Arcjet Accelerated Readiness Program, and the electrode configuration was already established going into the Arcjet ATTD program.[3] Integration testing began before 1990, when a development buck-regulated PCU demonstrated control of an arcjet.[5] The development tests under the Arcjet ATTD program focused instead on the PCU start circuit and flight packaging and the design of the ammonia PFS.

PCU Start-Circuit Testing

Development testing of the new start circuit focused on characterizing breakdown voltage as a function of cathode tip geometry, cathode gap, propellant flow rate, and start-circuit voltage rise rate.[11] As the pulse voltage rise rate was decreased, it was shown experimentally that the required breakdown voltage could be decreased. Essentially, more time at moderate voltages can be as effective in breaking down the arcjet gap as can a brief time at high voltages. At a lower rise rate, the blocking inductors saturate and close, effectively ending the start pulse, at a lower peak voltage. The electrical design had to trade between enlarging the blocking inductors to allow lower rise rates and designing the output insulation to handle higher voltages needed with high rise rates.

During these tests, Tilley et al.[10] showed that flow rate affected the breakdown voltage much more strongly than either cathode tip geometry or the gap between the cathode and the anode. This result allowed the possibility of further ensuring start reliability on-orbit by decreasing flow rate during the initial 85-A operation, and then ramping flow rate with output power over 60 s. Figure 6 shows the effect of both propellant flow rate and voltage rise rate on breakdown voltage from a later test with the flight geometry cathode. Note that

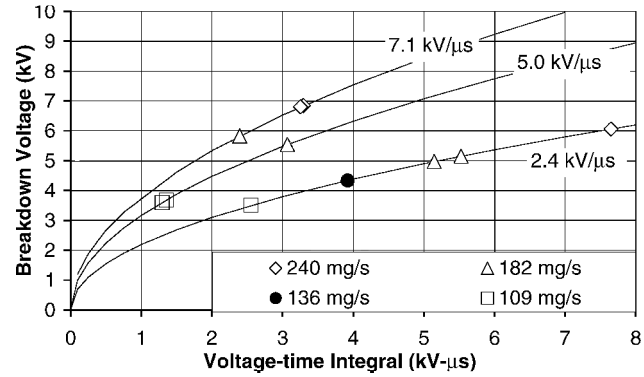

Fig. 6 Breakdown voltage as a function of flow rate and voltage rise rate.

breakdown voltages ranged from 3000 to 7000 V, well in excess of the 2500-V capability of the originally baselined start circuit. Because of this testing, the start-circuit requirements were redefined to be greater than 6000 V.

PFS Development Testing

To refine and validate the PFS concept, a development feed system was built and tested extensively.[12] These tests demonstrated the stability of the control system, allowed optimization of valve duty cycles, provided sizing of the sonic venturi, and established the operational sequence of the valves and heater power requirements. Most critically, these tests established the ability of the propellant feed system to provide purely gaseous ammonia vapor at the desired flow rates under any condition.

Initial Integrated Testing

In the spring of 1992, an arcjet thruster, the EM PCU and the development PFS were assembled for the first integrated demonstration test. The arcjet was started using the flight approach and operated at 26 kW with the design mass flow rate of 240 mg/s. The PCU provided the power, and the development PFS simultaneously supplied the ammonia to the arcjet during steady-state firings. The goals of this milestone test were met in demonstrating for the first time that the EMI from the arcjet and PCU had no effect on the operation of the PFS; full flow rate starts of the arcjet were feasible; the PFS start, stop, and control algorithms were fully compatible with the PCU and the arcjet; mass flow rate control of the PFS was better than the arcjet tolerance requirement; and there were no adverse interactions between arcjet operation and PFS flow control, for example, backflow oscillations.

EM Phase

The EM test sequence objective was to verify the operation of the flight designs of the arcjet/power cable, PCU, and PFS subsystems, first individually and then in combination. The sequence culminated in the integrated mission simulation (IMS) test, which integrated more components of the ESEX payload during an arcjet firing than at any other time in the ground testing.

Stand-Alone Tests

An EM arcjet and a power cable were fabricated and successfully completed functional and vibration tests at 9.3 *g* rms for 120 s in each axis. PCU stand-alone tests included verification of full power operation into a resistive load, arc ignition and operation of a development arcjet, EMI characterization, and three axes of vibration testing also at 9.3 *g* rms for 120 s each. Because of the integrated nature of the PFS with the ESEX structure, the performance of the PFS in vibration was verified by analysis at the component level and by test at the ESEX system level.

PFSEM Tests

All of the components of the PFS, including the tanks, transducers, line heaters, flow meter, and vaporizer, were integrated into

an EM configuration and tested over the mission duty cycle.[12] The control software was updated to a flight configuration, and flight configuration heaters were installed on the propellant and plenum tanks. Propellant line layouts and propellant tank coating were in a nonflight ground facility configuration.

With the PFS in a vacuum chamber, 11 outflows of at least 15 min were performed. The propellant tank was oriented so that liquid was always at the outlet until propellant depletion in the last outflow. This configuration allowed worst-case, as well as two-phase, testing of the system. Figures 7–9 present highlights of the 10th outflow. Figure 7 shows the pressure profile with a 120-s warmup sequence, followed by ~15.5 min of outflow. Aside from spikes associated with control valve cycling, the propellant tank pressure was steady at ~1400 kPa as long as liquid remained and then declined slowly during vapor outflow. Meanwhile, both plenum tank and arcjet pressures hold steady throughout both liquid and vapor outflow and the transition between them. Arcjet pressure equalizes with plenum pressure when the flow is off because the outflow isolation valve was positioned downstream of the arcjet pressure transducer for this test.

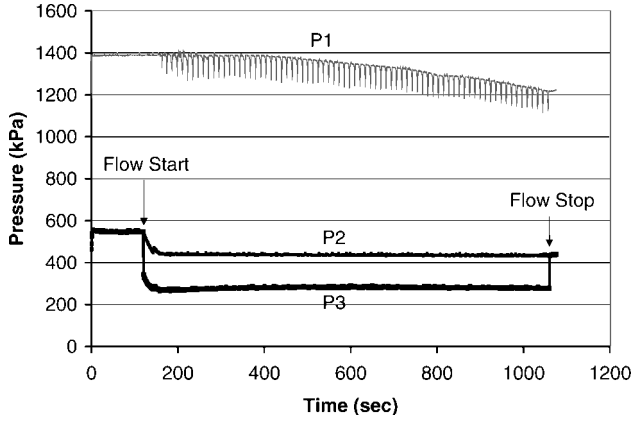

Fig. 7 PFS pressures during run 10.

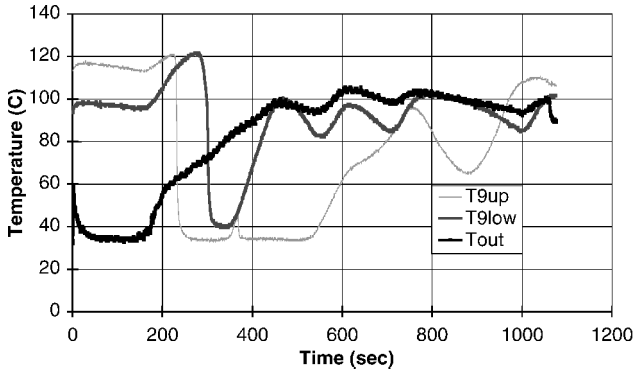

Fig. 8 Enhanced feedline heater temperatures, run 10.

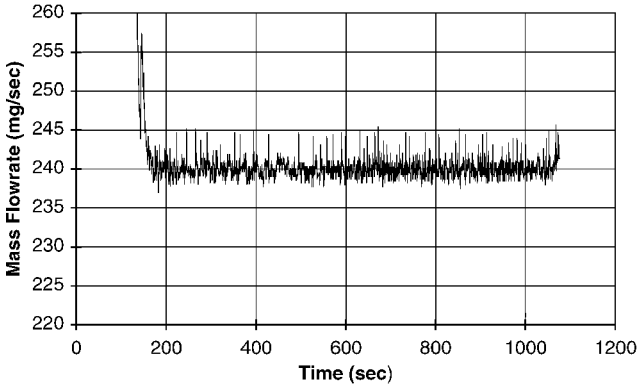

Fig. 9 PFS flow rate, run 10.

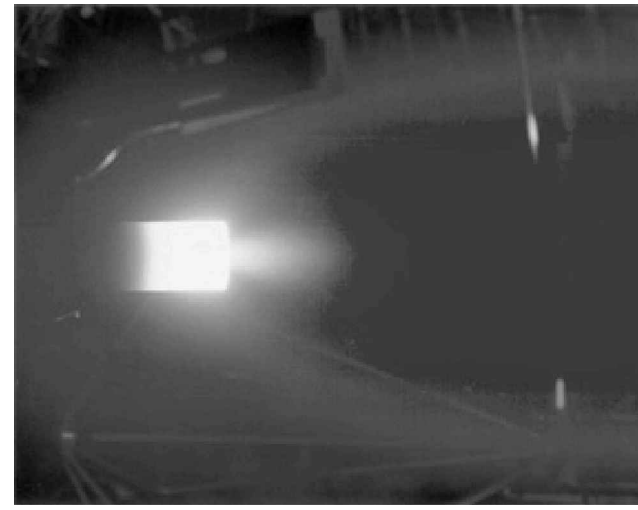

Fig. 10 EM arcjet during hot-fire testing.

Figure 8 shows the upper and lower vaporizer temperatures (T9up and T9low), which were used to control the upstream and downstream banks of vaporizer heaters, respectively. The upper temperature measurement shows 100% liquid outflow from the propellant tank until 550 s, as indicated by saturated liquid temperature of 35°C. This was followed by a rise in temperature to the control dead band during 100% vapor outflow from the propellant tank. The lower temperature measurement reflects downstream heater bank cycling. The temperature was controlled so that it never dropped to saturated liquid conditions at this location, ensuring full vaporization of the liquid. The vaporizer outlet temperature was continuously superheated throughout the outflow. Figure 9 shows that the mass flow rate, as measured by an independent mass flow meter, is controlled within 1.5% of nominal flow throughout the outflow that exceeded the requirement of 2.0%. The results confirmed that the design met the flow control requirements with margin.

Arcjet/PCU Performance Verification Test

The objective of this test was to measure the start, power ramp, and steady-state performance of the EM PCU and arcjet, operating together for the first time.[6,15] To facilitate thrust measurements, the PCU was mounted outside the vacuum cell with welding cables connecting the PCU and arcjet through the vacuum chamber wall and across the thrust stand. Five steady-state firings, 15 min in duration, demonstrated the complete operational sequence with no adverse interactions between the arcjet and PCU. Although two of the starts required a reduction to 75% of full propellant flow to achieve breakdown, this was determined to be due to the added capacitance of the long welding cables in the test setup and was not required later for the fully integrated PCU/arcjet tests. The arcjet thermal design successfully isolated the heat flux from the cable connector interface that had temperatures less than 65°C. The incandescent portion of the anode, shown firing in Fig. 10, was measured at 2000–2150 K. The PCU demonstrated that it met all requirements for efficiency and power control.

Figure 11 shows the thrust during the fourth firing, effectively reaching steady-state values within 120 s of the start and 70 s of reaching full power. The temperature profile validated that the 15-min time per arcjet ignition would be a sufficient test of steady-state operation. The specific impulse was measured to be 799 ± 17 s at an arcjet thrust efficiency of $27.2 \pm 1\%$. Figure 12 graphically illustrates all performance data taken. The shaded region represents the current, voltage, thrust, and flow measurement uncertainty. The regression line was generated from earlier ammonia arcjet data (shown by + symbols).[3] The acceptance test data point taken on the flight arcjet was shown by the × symbol. These data indicated good repeatability among three different arcjets with similar anodes running at nearly identical test conditions. It further showed that both the EM and flight arcjets met the performance requirements within the test uncertainty.

Arcjet/PCU Integrated Test

Following the performance test, the arcjet, cable, and PCU were integrated in the flight configuration within the vacuum cell to verify thermal compatibility of the arcjet/PCU combination and operation of the PCU in a vacuum. To prevent arcing inside the high-voltage portions of the PCU from vacuum pressures as high as 20 Pa when the arcjet was operating, the PCU was installed in a sealed and separately pumped enclosure. Five 15-min firings, for a total of 10 firings, in this test completed validation of the components for the full mission life requirements. The PCU thermal design demonstrated compatibility with the arcjet and adequate dissipation of heat from the power converters, inductors, and other components. In addition, with the cable in the integrated flight configuration, the arcjet was successfully started on each attempt at full propellant flow.

IMS

The final and most complex test of the EM sequence was the IMS.[15,16] The EM arcjet, PCU, PFS, batteries, and most of the diagnostics were tested in an integrated configuration for 10 firings of 15 min nominal duration. System compatibility between each component was evaluated based on issues such as reliable arc ignition and transition to full power with the batteries, proper flow control, power control, thermal distribution, and acceptable conducted and radiated EMI levels. In addition, a cold soak test was performed to verify the ability of the arc jet to start at the cold bias condition. The IMS also provided conducted and radiated EMI, video camera, radiometer, and solar cell data for use in the development of the ESEX diagnostics package.

The arcjet, power cable, PCU, and PFS were located inside the vacuum chamber, whereas the batteries were located outside the vacuum chamber to avoid internal arc discharge problems at the vacuum levels during arcjet firings. An insulated, liquid nitrogen cooled box controlled the battery temperature environment via active cooling at all times. The electrical power and grounding setup for the IMS was configured to duplicate the spacecraft configuration as closely as possible.

Table 2 provides an overall summary of the firings that were conducted in the IMS test sequence. The arcjet exhibited breakdown on each start pulse applied throughout the testing. No problems were noted with the transition from ignition to steady state, and the PFS consistently provided stable outflows to the arcjet.

After an initial run with the PCU powered by a facility power supply and the arcjet using the laboratory ammonia system, the system was reconfigured with the batteries providing power to the PCU and the PFS providing propellant to the arcjet. The first, fifth, and eighth battery firings shut down prematurely due to a fine-line separation problem on the circuit card assemblies in the EM PCU. This problem was known and was corrected in the flight unit before the start of the IMS. Aside from the failure of a preproduction hybrid FET, all other firings were conducted successfully. Finally, a cold thruster test was performed after the final IMS battery test firing to retire a concern of ammonia condensing in the thruster passages. The arcjet was cooled with dry ice to −28°C and started without a problem, eliminating the need for a special arcjet heater to avoid condensation.

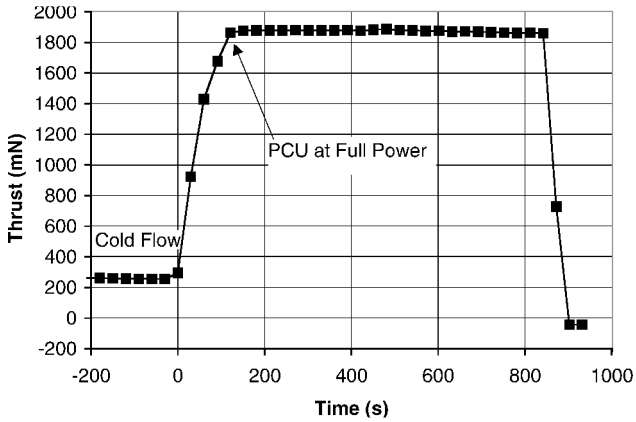

Fig. 11 EM arcjet thrust profile (run 4).

Table 2 Summary of IMS firings

Run	Designator	Duration, min	Comments
1	Rapid checkout	10	Final checkout before battery firing
2	1st Battery firing	8	Shut down prematurely, suspect PCU interlayer fine-line board separation
3	2nd Battery firing	15	Started with PCU at −26°C
4	3rd Battery firing	15	Started with PCU at −21°C
5	4th Battery firing	15	Started with PCU at −7°C
6	5th Battery firing	11	Started with PCU at +4°C, shutdown occurred again
7	6th Battery firing	15	Started with PCU at −18°C
8	7th Battery firing	16.5	Took EMI data
9	None	0	Short through PCU discovered, no firing attempted
10	8th Battery firing a	3.5	PCU was not uniformly cooled before firing, shutdown occurred
11	8th Battery firing b	19	PCU cooled to −18°C, took EMI data inside cell
12	9th Battery firing	17	Did not start on first attempt, reduced flow to start, EMI data taken
13	10th Battery firing	18	Rough start, but start at full flow first time; shut down when battery below 150 V
14	Cold thruster test	1	Demonstrated cold soak start capability

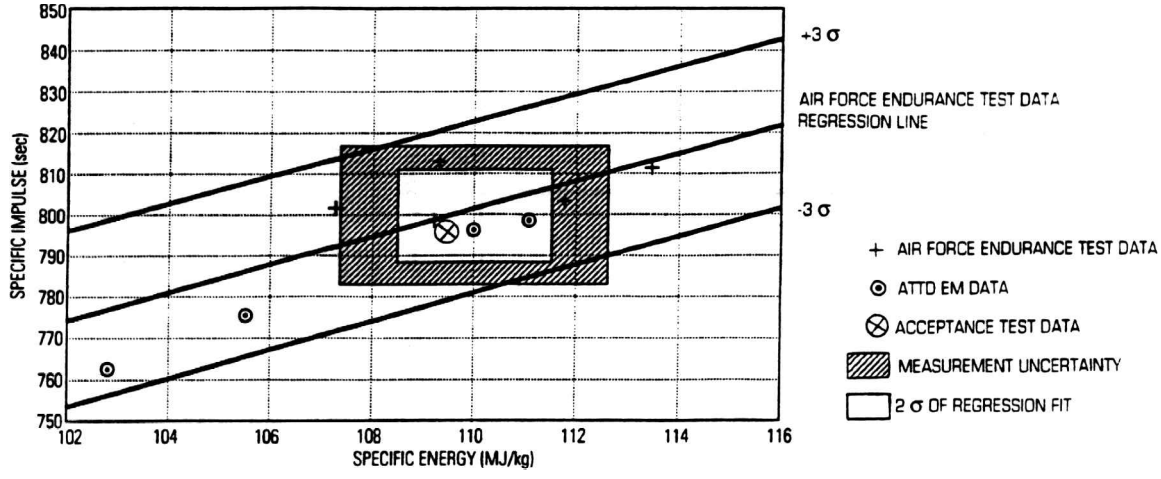

Fig. 12 EM arcjet performance test results.

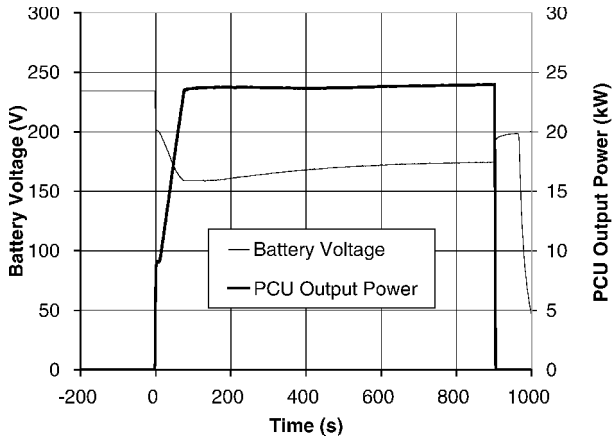

Fig. 13 Battery voltage and PCU output power during IMS firing 3.

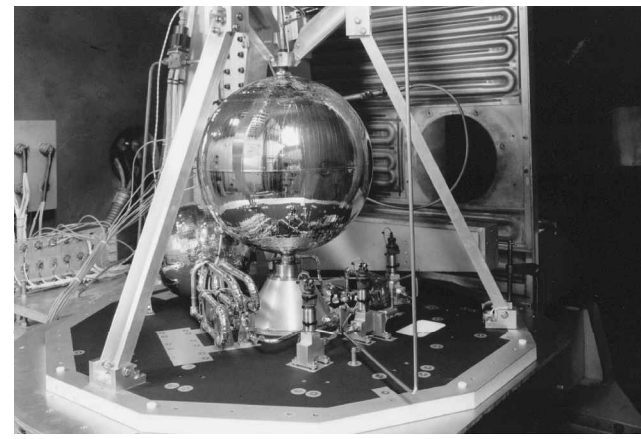

Fig. 14 Flight PFS in test.

Figure 13 shows the battery voltage input to the PCU and the PCU output power during one of the 15-min runs. Following ignition, there was a rapid ($\ll$1 ms) drop in battery voltage from 235 to about 210 V. Battery current would rise after about 15 ms to about 40 A and then to 60 A over the next 3–4 s, while the voltage decayed slightly to about 190 V. The output power was held at about 10 kW for the next 10–12 s until it was ramped for approximately 60 s, during which the battery voltage decayed further to between 160 and 165 V. After dropping to approximately 160 V as the 26-kW power level was reached, the voltage would recover throughout the run due to internal heating of the batteries. Following shut down with the load removed, battery voltage would recover to nearly 200 V and continue to climb slowly again due to heating.

The IMS demonstrated, for the first time, the successful integrated operation of these subsystems with flight-type batteries. The PCU demonstrated the ability to start the arcjet and transition to steady-state power using input battery power. The PFS was shown to supply stable, single-phase vapor flow at the proper flow rate with the arcjet firing. The batteries were shown to tolerate an accelerated charge cycle, as long as temperature was controlled.

Flight Unit Tests

The acceptance testing objectives were to verify if the flight PCU and arcjet would tolerate the launch vibration levels, thrust performance of the flight arcjet, operation of PCU under temperature extremes, operation of the flight PFS, and to perform calibration of the venturi flow meter in the PFS. The tests in the sequence were as follows: arcjet and power cable vibration testing, arcjet performance verification, integrated arcjet/cable/PCU firings, PCU vibration testing, and PCU/PFS integrated tests. Nonoperational acceptance requirements, such as proof pressures, leak rates, dielectric strengths, insulation resistances, and electrical bonding were verified before and after major testing.

The arcjet, power cable, and receptacle vibration test was completed without damage or effect on operation. The arcjet had stable operation at 26 kW with voltages ranging from 106 to 111 V over the three firings, compared to a specified value of 110 ± 25 V. The arcjet performance met the 800-s specific impulse requirement within experimental uncertainty, as shown in Fig. 13.

The flight arcjet and power cable underwent random vibration to an overall level of 9.3 *g* rms for 60 s on each of three axes before performance and integrated firings. The flight PCU was later vibrated separately to the same levels. Postvibration operation of the PCU was verified on a resistive load. During the performance verification firing, the PCU was mounted outside the test cell to allow thrust measurements, and the arcjet was fired for 15 min. In the two integrated arcjet/cable/PCU firings, the arcjet, power cable, and PCU were all mounted inside the vacuum chamber. The firings were conducted at -29 and $+55^{\circ}$C, respectively, to simulate extreme cold and hot spacecraft conditions. For both the performance verification and the integrated firings, the facility ammonia supply was used in place of the flight PFS, which was still being fabricated.

The PCU/PFS integrated test was identical to that performed in the EM sequence, with the PCU controlling the arcjet valve and conditioning the pressure signals. The PFS was mounted inside the vacuum chamber, as shown in Fig. 14. Calibration of the PFS flow meter was accomplished by passing the PFS outflow through an independent, laboratory mass flow meter. Outflows of 15 min were conducted at flow rates of 220, 240, and 260 mg/s. In addition, outflows were performed to verify operation over the 24–33 V specified range of heater voltages.

Summary

The ESEX program developed the first flight arcjet design at the 26-kW power level, including significant thermal and structural design innovations, materials joining technology, and high-power electrical passthrough design. A robust 30-kW PCU was built that set a record for 1999 for the power density of a flight electronics box, as well as on-orbit processing power. The robustness of the design was demonstrated on-orbit as the PCU continued to operate even as the battery pack degraded and the input voltage to the PCU fell well below the specified 160-V minimum. Faced with the problem of not being able to recreate the LES 8/9 ammonia PFS, a flow system was designed to take advantage of existing resources and innovative zero-*g* fluid handling techniques to build a very capable feed system. Operation on-orbit verified the thermocapillary design, and the only surprise came when a section of the line became cooler than expected and condensed propellant. That data actually served as further confirmation of the ability to move the liquid propellant to a preferred location using differential heating of the tanks and lines.

The ultimate measure of the success of a ground-testing program is successful on-orbit hardware performance. In the case of the ESEX arcjet propulsion subsystem, all components performed as expected. Beyond the on-orbit success of the arcjet hardware, this program made other contributions. Data were gathered and technology developed to deal with high heat loads in the proximity of a spacecraft that will be useful for future high-power electric propulsion (EP) missions now being contemplated. Power conditioning techniques that will be applicable to other EP technologies up to tens or even hundreds of kilowatts were demonstrated. Most significant, it was shown that a large switching power supply can be accommodated in a small enclosure and be made EMI/EMC compatible with other spacecraft electronics and even with logic circuitry inside the same enclosure. This will be a critical stepping stone to building even larger power conversion systems for the future. Finally, the testing program itself established a template that can be followed by future large, high powered EP systems. The demonstration of elements of the propulsion subsystem in integrated tests even at the breadboard level caught many problems at an early stage that allowed for their resolution in advance of the flight hardware testing. The use of a more packaged EM design for early testing provided better fidelity to the actual flight design. Overall, the approach provided an effective means to drive out risk items and resulted in a flight design that met all mission objectives.

Acknowledgments

The authors would like to acknowledge the close teamwork and support during the hardware development phase of the program of personnel from TRW, especially Mary Kriebel, and the Air Force Research Laboratory, especially Daron Bromaghim. The authors gratefully acknowledge the consistent team contributions of John Hamley of NASA John H. Glenn Research Center at Lewis Field for many power conditioning unit issues, particularly the suggestion to use the pulser start circuit.

References

[1]Bromaghim, D. R., LeDuc, J. R., Salasovich, R. M., Spanjers, G. G., Fife, J. M., Dulligan, M. J., Schilling, J. H., White, D. C., and Johnson, L. K., "Review of the Electric Propulsion Space Experiment Program," *Journal of Propulsion and Power*, 2002; also AIAA Paper 99-2706, June 1999.

[2]Kriebel, M., "System Engineering, Design, Integration, and Qualification of Electric Propulsion Space Experiment Flight Unit," *Journal of Propulsion and Power*, 2002.

[3]Lichon, P. G., and Cassady, R. J., "Performance Improvement of 26-kWe Ammonia Arcjet," AIAA Paper 90-2532, July 1991.

[4]Polk, J. E., Goodfellow, K. D., and Pless, L. C., "Ammonia Arcjet Engine Behavior in a Cyclic Endurance Test at 10 kW," International Astronautical Federation, IAF Paper 92-0612, Sept. 1992.

[5]Vaughan, C. E., Cassady, R. J., and Fisher, J. R., "Design, Fabrication and Test of a 26 kW Arcjet and Power Conditioning Unit," International Electric Propulsion Conf., IEPC Paper 93-048, Sept. 1993.

[6]Wong, S. P., "Testing of 30 kW Arcjet PCU with Arcjet Thrusters," International Electric Propulsion Conf., IEPC Paper 91-070, Oct. 1991.

[7]Fisher, J. R., and Meyer, S. D., "Design and Development of the MR-510 Arcjet Power Conditioning Unit," AIAA Paper 98-3630, July 1998.

[8]Lynn, P. J., Osborn, M. F., Sankovic, J. M., and Caveny, L. H., "Electric Propulsion Demonstration Module (EPDM) Flight Hall Thruster System," International Electric Propulsion Conf., IEPC Paper 97-100, Aug. 1997.

[9]Polk, J. E., Kakuda, R. Y., Anderson, J. R., Brophy, J. R., Rawlin, V. K., Patterson, M. J., Sovey, J., and Hamley, J., "Validation of the NSTAR Ion Propulsion System on the Deep Space One Mission: Overview and Initial Results," AIAA Paper 99-2274, June 1999.

[10]Tilley, D. L., McFall, K. A., Castillo, S., Andrews, J. C., and Bromaghim, D. R., "An Investigation of the Breakdown Voltage Characteristics of a 30-kW Class Ammonia Arcjet," AIAA Paper 93-1901, June 1993.

[11]Aadland, R. S., Vaughan, C. E., Hoskins, W. A., and Kay, R. J., "Achieving Reliable, Repeatable Starts of a 26 kW Arcjet," International Electric Propulsion Conf., IEPC Paper 93-049, Sept. 1993.

[12]Vaughan, C. E., and Morris, J. P., "Propellant Feed Subsystem for a 26-kW Flight Arcjet Propulsion System," AIAA Paper 93-2400, July 1993.

[13]Ostrach, S., "Low Gravity Fluid Flows," *Annual Review of Fluid Mechanics*, Vol. 14, 1982, pp. 313–345.

[14]Ostrach, S., "Convections due to Surface Tension Gradients," *Proceedings of the 21st Plenary Meeting of COSPAR*, Innsbruck, Austria, May-June 1979.

[15]Aadland, R. S., Vaughan, C. E., Cassady, R. J., and Kay, R. J., "Integrated Mission Simulation of a 26-kW Flight Arcjet Propulsion System," AIAA Paper 93-2395, July 1993.

[16]Cassady, R. J., Hoskins, W. A., and Vaughan, C. E., "Qualification of a 26-kW Arcjet Flight Propulsion System," AIAA Paper 95-2505, July 1995.